OXYGEN SENSOR WITH ADVANCED OXIDE ELECTRODE MATERIALS

P. Shuk, R. Jantz and H.-U. Guth*
Rosemount Analytical Inc.
Emerson Process Management
6565 Davis Industrial Parkway
Solon, OH, USA
Emails: Pavel.Shuk@Emerson.com
*Dresden University of Technology
Department of Chemistry, Bergstrasse 66c
D-01069 Dresden, Germany

In Memory of our beloved teacher, colleague, and friend,
Professor Hans-Heinrich Möbius

Submitted: Feb. 15, 2012 ***Accepted: Feb. 23, 2012*** ***Published: Mar. 1, 2012***

Abstract- Calcium doped lanthanum and yttrium manganite electrode materials with oxygen deficiency and low polarization resistance (<30Ω*cm^2 at 600°C) were tested in new advanced electrochemical sensor for the oxygen measurements. Oxygen sensor with oxide electrodes was showing fast response

(t_{95}~5s at 600°C), good reproducibility (±0.04% O_2) and long term stability at different oxygen concentration.

Index terms*:* oxygen concentration measurements, potentiometric gas sensor, oxide electrode, perovskite structure, rare earth manganite electrode, combustion application.

I. INTRODUCTION

Electrochemical oxygen sensors based on zirconia solid electrolytes widely used today in different industrial applications and for controlling fuel/air ratio in internal combustion engines (lambda sensor) were first introduced 40 years ago by Peters and Möbius [1] and Weissbart and Ruka (Westinghouse) [2]. Most industrial zirconia oxygen sensors are based on electrochemical cell with stabilized zirconia solid electrolytes working in potentiometric mode [3-6]. This electrochemical cell consists of zirconia solid electrolyte (mostly yttrium stabilized zirconia, YSZ) and two platinum electrodes printed and sintered on the opposite sides of zirconia ceramics and exposed to the process and reference gases:

$$O_2(p_{O_2}, ref), Pt \mid Zirconia \mid Pt, O_2(p_{O_2}, process) \quad (1)$$

With the reference side gas tight separated from the process side an e.m.f., E, will be developed according to the Nernstian equation:

$$E = C + \frac{RT}{4F} \ln \frac{p(O_2)_{process}}{p(O_2)_{ref}} \quad (2)$$

with constant C related to the thermal junctions in the probe and reference/process sides temperature and pressure slight mismatch, R universal gas constant, T the process temperature in °K and F the Faraday number.

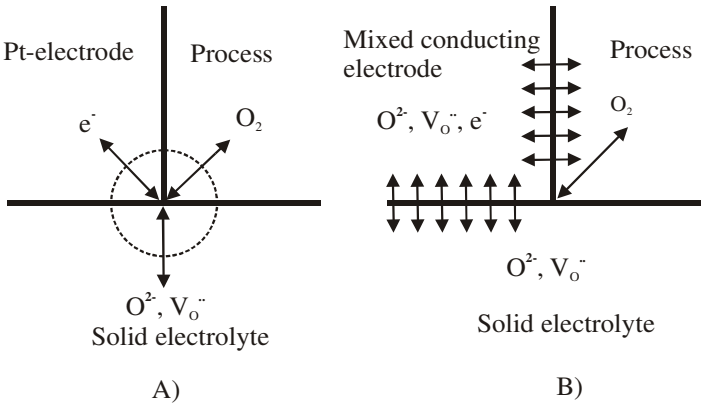

$$O_2(gas) \leftrightarrow O_2(Electrolyte/Electrode)$$
$$O_2(Electrolyte/Electrode) \leftrightarrow 2O(Electrolyte/Electrode)$$
$$2O(Electrolyte/Electrode) \leftrightarrow 2O(Electrolyte/Electrode/Gas)$$
$$2O(TPB) + 4e^{'}(Electrode) + 2V_O^{\cdot\cdot}(Electrolyte) \leftrightarrow O_O(Electrolyte)$$

Figure 1. Oxygen reaction on the triple phase boundary (TPB)

The oxygen reaction is taking place on the triple phase boundary (TPB): electrode, electrolyte and gas phase where oxygen molecules, O_2, electrons, e'; and oxygen vacancies, $V_O^{\cdot\cdot}$; are available (Figure 1A) and includes molecular oxygen absorption, dissociation on the electrolyte/electrode surface and final diffusion to TPB where oxygen electrochemical reaction will take place. This electrochemical reaction is limited by the TPB region but using composite electrode with electronic and ionic conductors, e.g., Pt-Zirconia or mixed ionic-electronic conductive electrode electrochemical reaction will be extended to the electrode bulk and electrochemical gas sensor performance will be highly improved (Figure 1B).

The platinum and platinum composite electrodes are the mostly used in electrochemical cells because of their chemical stability in oxidizing and reducing environment and high catalytic activity for the electrochemical oxidation or reduction reaction. For the electrochemical reaction a potentially good electrode material would be a mixed electronic-ionic conductor with the oxygen. exchange not limited to the three electrode/electrolyte/gas phase contact region [6]. The binary exchange not limited to the three electrode/ electrolyte/gas phase contact region. The binary oxides with perovskite structure $Ln_{1-x}M_xBO_3$ (B=Co, Ni, Mn, Fe, Cr; M= Sr, Ca, Mg) are the most promising mixed conducting materials and have been intensively investigated in the past as electrode materials in different electrochemical cells, i.e., solid oxide fuel cells, electrolysers and sensors [7-10]. Among perovskite oxides rare earth manganites, $LnMnO_3$ with high chemical

stability, electrical conductivity over 200 S/cm and thermal expansion coefficients (TEC) similar to the stabilized zirconia attract the most attention [11] and were finally implemented in high temperature solid oxide fuel cells cathodes [12].

Thermodynamic investigations on $LaMnO_3$ show that the oxygen vacancies are not the major nonstoichiometry defects in the oxidizing atmosphere and mangatites electrode application at lower temperature would require to enhance oxide ion conductivity beyond that due to the nonstoichiometry [13]. In order to develop new active electrode materials based on manganites we investigated in the past Co and Ni doped $La(Sr)MnO_3$ [14-15]. It was found a shift in stochiometry towards oxygen deficient composition in particular at low oxygen partial pressure and significant increase in ionic conductivity. Unfortunately Co/Ni substitution would be reducing lanthanum manganite stability and increasing thermal expansion coefficients to $12x10^{-6}/K^{-1}$ making application with zirconia solid electrolyte (TEC= $10x10^{-6}K^{-1}$) in temperature changing environment unacceptable even after several thermal cycling. Calcium substitution in lanthanum or yttrium manganite was shown in the past to be more preferable in creating oxygen deficiency [11, 16].

In this paper we explore oxygen deficient calcium substituted lanthanum and yttrium manganites with the highest conductivity and thermal expansion coefficients close to zirconia ceramics as electrode materials in electrochemical oxygen sensors based on zirconia solid electrolytes.

II. EXPERIMENTAL

$La_{0.7}Ca_{0.3}MnO_{3-\delta}$ and $Y_{0.5}Ca_{0.5}MnO_{3-\delta}$ were prepared using the Pechini method, starting from precursors La_2O_3, $CaCO_3$ and $MnCO_3$ or Y_2O_3, $CaCO_3$ and $MnCO_3$. The phase composition of the prepared doped lanthanum and yttrium manganites was confirmed using X-ray diffraction. The room/high temperature powder X-ray diffraction patterns (PXD) of the ultrafine powders were obtained with a SCINTAG PAD V diffractometer equipped without/with a high temperature attachment with monochromatized $CuK\alpha$ radiation at a 2θ scan of 0.5°/min. Cell parameters were calculated by fitting the observed reflections with a least-squares program. The reflection from the (422) plane was used for the determination of average crystallite size. The average crystallite size, D, of the prepared powders was calculated from the Scherrer formula:

$$D = \frac{0.9\lambda}{\beta\cos\theta} \quad (3)$$

where λ is the wavelength of the X-rays, θ is the diffraction angle, $\beta = \sqrt{(\beta^2_m - \beta^2_s)}$ is the corrected halfwidth of the observed halfwidth, β_m, of the (422) reflection in samples of manganite, and β_S is the halfwidth of the (422) reflection in a standard sample (D ~ 100 nm).

For the electrical conductivity measurements the manganite samples were pre-pressed uniaxially, then isostatically under 500 MPa. The green densities were about 50%. The green pellets were sintered at 1150-1250ºC for 1 h with a programmed heating and cooling rate of 5ºC/min.

Calcium substituted lanthanum or yttrium manganite powders were ball milled in ethanol for 24 h and mixed with an appropriate amount of organic binder and solvent to prepare manganite paste. This manganite paste was used to print process electrode on one side of zirconia disk and sintered at ~1250-1300°C for 2 h. Platinum reference electrodes were prepared by printing commercial Pt-paste (Heraeus Inc., PA, USA) on other side of zirconia disk followed by sintering at ~1100°C for 2 h. The area of manganite electrode was ~0.8 cm^2 and of Pt-reference electrode ~1.5 cm^2. Zirconia disks with process manganite and reference Pt-electrode were brazed into E-Brite tube assembly with flange using standard vacuum brazing procedure for the process and reference gas regions separation. The impedance measurements were performed with an Impedance Analyzer SI-1260 (Solartron Instruments) over 0.01 Hz to 1 MHz frequency range at 350-500ºC up to 650ºC. The inductive error associated with various components of the measurement circuit was evaluated by carrying out measurements in the rig on reference resistances in place of samples. All the measurements were corrected accordingly. The curve fitting was done with "Zview 2.1b" with different equivalent circuits.

Test gas mixtures were prepared using Environics 4000 gas mixing system (Environics, Inc., CT, USA) and OXT 4000 Oxygen Analyzer (Rosemount Analytical Inc., OH, USA) was implemented using calibration port to control oxygen mixtures composition. For the data acquisition we used hardware from National Instruments, which included signal conditioning module (SCXI-1000+SCXI-1102 card) and the plug-in DAQ card (AT-MIO-16 XE-50).

A special designed sensor test setup includes gas preheated line delivering fixed amount of gas mixture to the sensor chamber (Figure 2). The gas flow rate was kept constant at 2.5 L/h. Gas delivery line outside the sensor package was heated to ~130ºC to prevent moisture condensation.

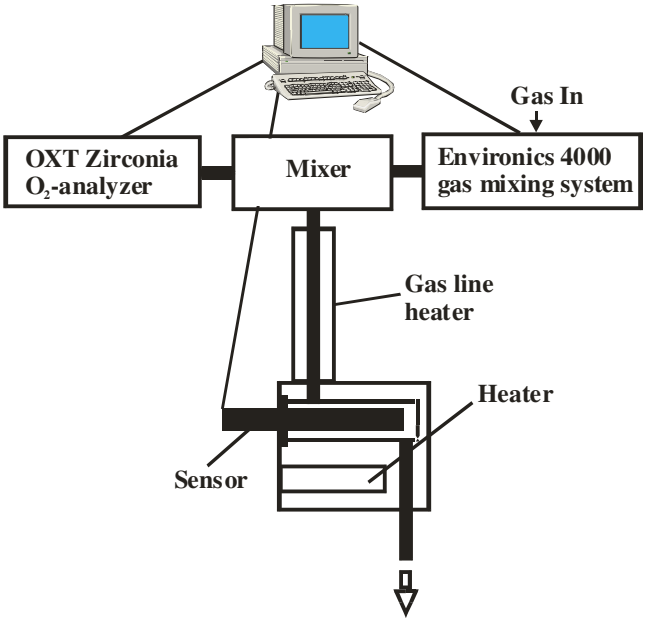

Figure 2. Oxygen sensor test setup

III. RESULTS

X-ray investigations shown formation of cubic perovskite structure for $La_{0.70}Ca_{0.30}MnO_{2.975}$ with lattice parameter a=0.3875±0.0005 nm and orthorhombic perovskite structure for $Y_{0.50}Ca_{0.50}MnO_{2.985}$ with lattice parameters a=0.5300, b=0.5460 and c=0.7440±0.0005 nm. The average crystallite size of calcium doped manganites powders, calculated by the Scherrer formula from the PXD data was between 40 to 60 nm. The fine manganites powders were sintered into pellets with apparent densities over 94 % of the theoretical value at 1150-1200°C, whereas these manganites, prepared by conventional ceramic techniques would require ~150-200°C higher temperature for the complete sintering. Temperature dependent X-ray diffraction measurements show no transformation of the perovskite structure nor phase separation even after annealing at 1000°C for 2 weeks.

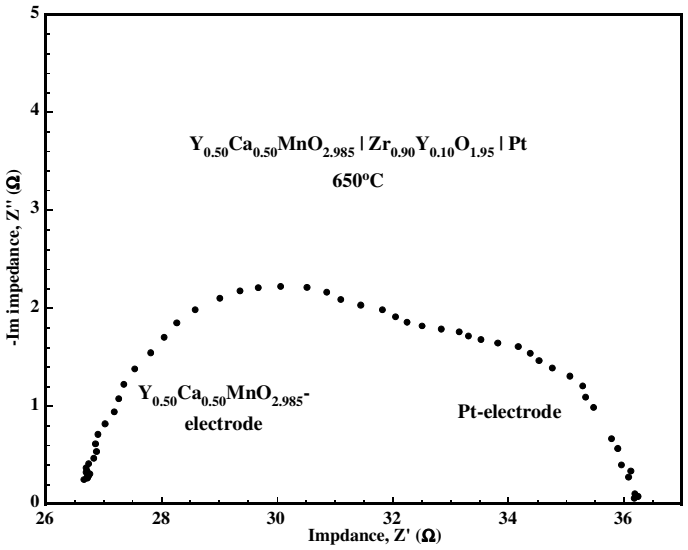

Figure 3. The complex impedance plot at 650°C for the cell: air, $Y_{0.50}Ca_{0.50}MnO_{2.975}$ | $Zr_{0.9}Y_{0.1}O_{1.95}$ | Pt, air

In figures 3-5 are shown some typical impedance spectra of $La(Y)_{1-x}Ca_xMnO_{3-\delta}$| $Zr_{0.9}Y_{0.1}O_{1.95}$ |Pt cell interfaces at different temperatures. At elevated temperatures polarization of manganite electrodes is similar to the commercial Pt electrodes and is negligible (Figures 3-4). By reducing the temperature as expected a significant polarization of Pt-electrode was observed but much less on the manganite electrodes (Figure 5). Electrochemical reduction or oxidation of molecular oxygen on the metallic electron conducting electrode film like platinum is only limited to the areas with oxide ions availability on the triple phase boundary close to zirconia solid electrolyte surface (Figure 1a) contributing to the high electrode polarization at lower temperatures because of slowing down diffusion, absorption and oxygen electrochemical reaction limited to TPB. Based on the chemical analysis of the calcium substituted manganite materials quenched from the

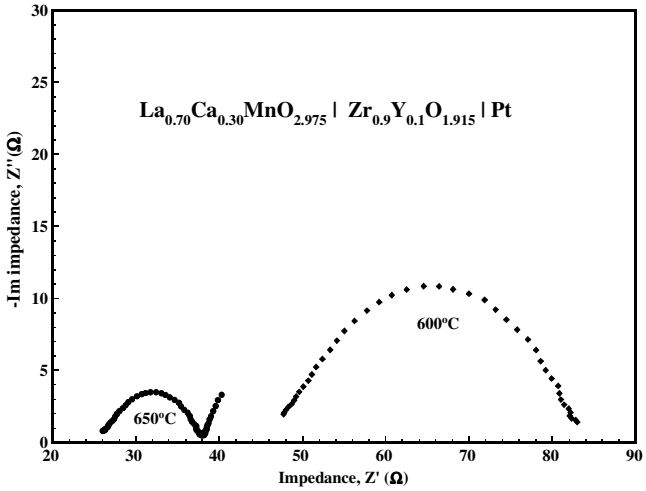

Figure 4. The complex impedance plot at 600 and 650°C for the cell: air, $La_{0.70}Ca_{0.30}MnO_{2.975}$ I $Zr_{0.9}Y_{0.1}O_{1.95}$ I Pt, air

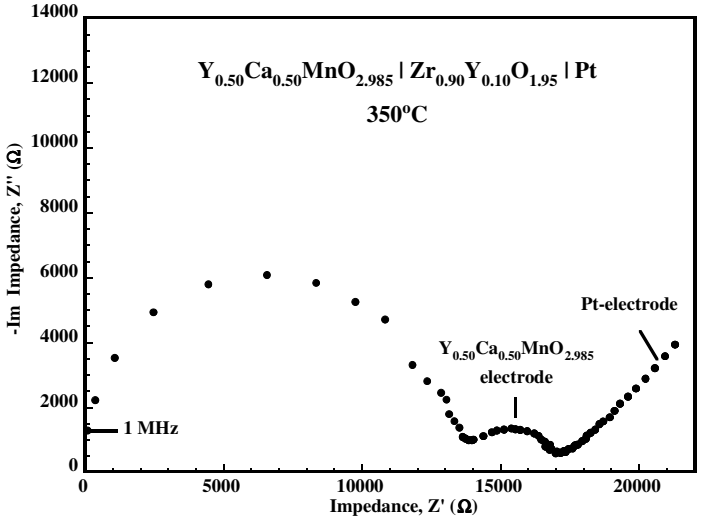

Figure 5. The complex impedance plot at 350°C for the cell: air, $Y_{0.50}Ca_{0.50}MnO_{2.985}$ I $Zr_{0.9}Y_{0.1}O_{1.95}$ I Pt, air

high temperature significant amount of oxygen vacancies is forming according the reaction (Kröger-Vink notation) [11]:

$$2Mn_{Mn}^{\cdot} + O_O^x = 2Mn_{Mn}^x + V_{\ddot{O}} + \frac{1}{2}O_2 \quad (4)$$

where $Mn_{Mn}^{\cdot}$ is Mn^{4+}, Mn_{Mn}^x is Mn^{3+}, O_O^x is O^{2-} and $V_{\ddot{O}}$ is oxygen vacancy.

Oxygen vacancies formed at manganite electrode/zirconia solid electrode interface will propagate, extending the reactive sites for the molecular oxygen reduction/oxidation reaction into manganite electrode bulk. Electrochemical activity of the electrodes will be highly enhanced reducing the electrode polarization especially at the lower temperatures.

Polarization resistance of calcium doped manganite electrodes as well as ionic conductivity of zirconia solid electrolyte calculated from impedance spectra at different temperatures are summarized in figure 6. Manganite electrodes polarization resistance was 1-2 orders of magnitude smaller that Pt-electrode at lower temperatures, e.g., 400°C.

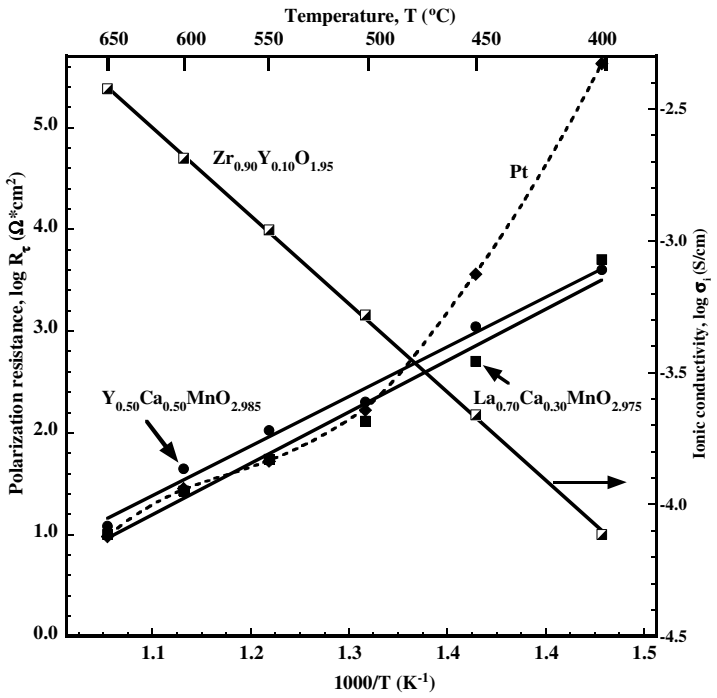

Figure 6. Temperature dependence of manganite electrodes polarization resistance and ionic conductivity of $Zr_{0.9}Y_{0.1}O_{1.95}$

Oxygen sensor with calcium doped manganite process and reference electrode was tested in different combustion environment with oxygen concentration variation between 2 and 20%. As it can be seen from figure 7 even at relative lower temperature, 600°C oxygen sensor with calcium substituted manganite electrode remains highly sensitive to the oxygen concentration change between 2 and 20% O_2. Response time (95%) was just several seconds with stable sensor signal reading in 20-25 s. Reproducibility test was performed in 2…5% O_2 concentration range

covering most of combustion process applications. As it can be seen from figure 8 oxygen sensor with oxide electrodes reproducibility was better than 0.04% O_2 and was symmetrical to the reducing or increasing O_2 concentration.

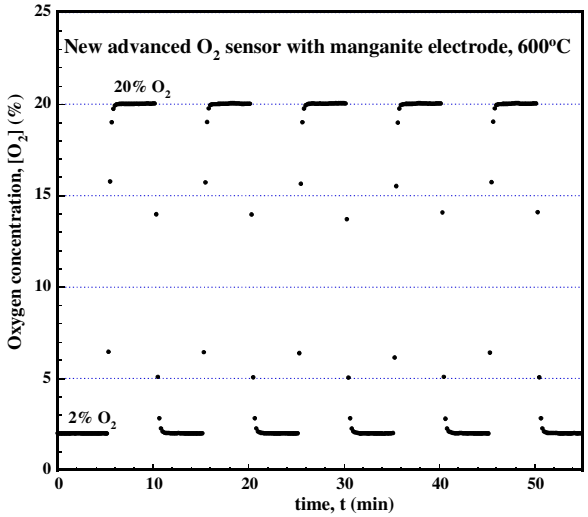

Figure 7. O_2 sensor with manganite electrode response at 2 & 20% O_2

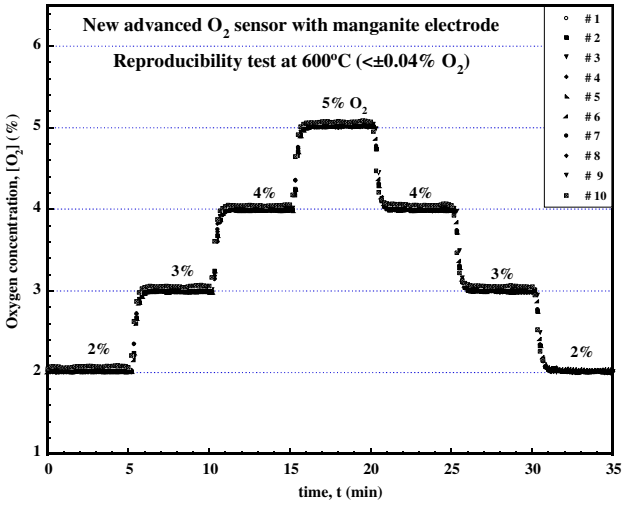

Figure 8. O_2 sensor with manganite electrode reproducibility test in 2…5% O_2 range

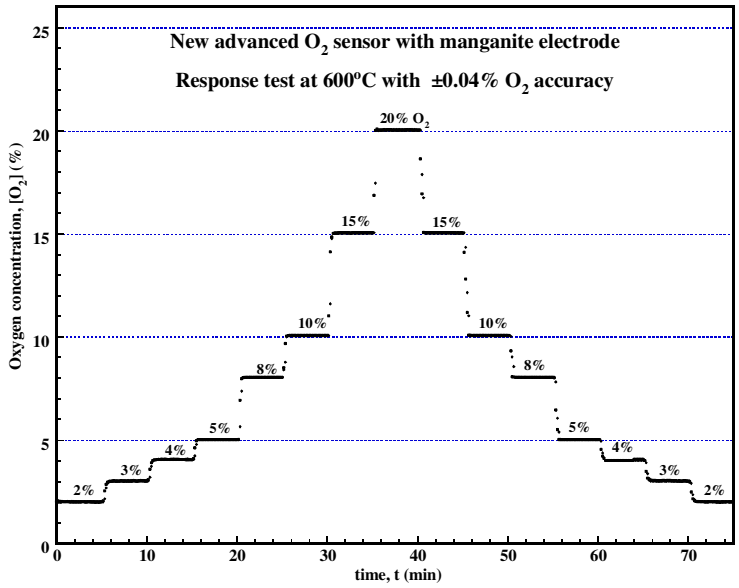

Figure 9. O_2 sensor with manganite electrode response in 2…20% O_2 range

Finally, new advanced O_2 sensor with doped manganite electrodes was tested in 1…2% O_2 concentration steps covering 2…20% O_2 combustion range as well as for the stability at very common for the combustion 2.5% O_2 concentration. As it can be seen from figure 9 response of the new advanced O_2 sensor with oxide electrodes was reproducible and accurate (±0.04% O_2) at all investigated O_2 concentrations. Stability test didn't show any oxide electrode degradation issues after over 1000 hours testing (figure 10).

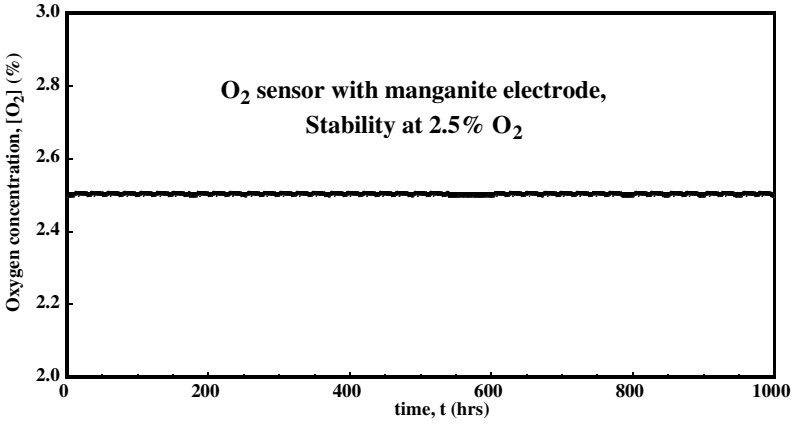

Figure 10. Advanced O_2 sensor with manganite electrode stability test at 2.5% O_2

IV. CONCLUSION

New advanced oxygen sensor based on zirconia solid electrolyte was developed and tested using oxide electrodes with perovskite structure. Calcium doped lanthanum and yttrium manganite electrodes with oxygen deficiency were showing better polarization resistance compare to commercial Pt-electrode especially at lower temperatures (~27 $\Omega*cm^2$ at 600°C). New oxygen sensor with mixed electron and oxide ion conducting manganite electrodes was showing fast response (t_{95}~5s at 600°C), good reproducibility in wide oxygen concentration range (±0.04% O_2) and any drift issues in the long term stability test.

ACKNOWLEDGMENT

The authors would like to thank Dr. Guerman Popov (now with University of Waterloo, Canada) for the oxide electrode materials preparation and helpful discussion.

REFERENCES

[1] H. Peters, H.-H. Möbius, "Procedure for the gas analysis at elevated temperatures using galvanic solid electrolyte elements", DD-Patent 21673, August 1961.

[2] J. Weissbart, R. Ruka, „Oxygen gauge", Rev. Sci. Instrum., vol. 32, pp. 593-595, May 1961.

[3] H.-H. Möbius, "Solid state electrochemical potentiometric sensors for gas analysis", in Sensors a comprehensive survey, vol. 3, W. Göpel, J. Hesse, J. N. Zemel, Eds. New York: VCH, pp. 1105-1154, 1992.

[4] W. C. Maskell, "Progress in the development of zirconia gas sensors", Solid State Ionics, vol. 134, p. 43-50, January 2000.

[5] S. Zhuiykov, Electrochemistry of zirconia gas sensors, Boca Raton/London/New York: CRC Press, 2008.

[6] P. Shuk, "Process Zirconia Oxygen Analyzer: State of Art", Technisches Messen, vol. 77, No 1, pp. 19-23, January 2010.

[7] L.G. Tejuca, J.L.G. Fierro, Properties and applications of perovskite-type oxides, New York: Marcel Dekker, 1993.

[8] P. Shuk, “Contribution to the noble metal free electrochemical cells development”, Habilitationscript, Greifswald University, Germany, December 1992.

[9] P. Shuk, A. Vecher, V. Kharton, L. Tichonova, H.-D. Wiemhöfer, U. Guth, W. Göpel, “Electrodes for oxygen sensors based on rare earth manganites and cobaltites”, Sensors and Actuators, vol. B15-B16, pp. 401-405, October 1993.

[10] J.W. Fergus, “Perovskite oxides for semiconductor-based gas sensors”, Sensors and Actuators, vol. B123, pp. 1169-1179, May 2007.

[11] P. Shuk, L. Tichonova, U. Guth, “Materials for electrodes based on rare earth manganites”, Solid State Ionics, vol. 68, pp. 177-184, March 1994.

[12] T. Ishihara, Perovskite Oxide for Solid Oxide Fuel Cells, New York: Springer, 2009.

[13] H.U. Anderson, "Review of P type doped perovskite materials for SOFC and other applications", Solid State Ionics, vol. 52, pp. 33-41, May 1992.

[14] P. Shuk, K. Künstler, W. Richter, U. Guth, L. Tichonova:, “Mixed ionic-electronic conductors on the basis of calcium doped lanthanum manganites”, in Solid State Phenomena, W. Bogusz, W. Jakubowski, F. Krok, Eds, Aedermannsdorf: Scitec, vol. 39-40, pp. 103-106, May 1994.

[15] P. Shuk, U. Guth, “Mixed conductive electrode materials for SOFC and oxygen sensors”, Ionics, vol. 1, pp. 106-111, February 1995.

[16] F. Licci, G.Turilli, P. Ferro, “Determination of mamganese valence in complex La-Mn perovskites”, J. Magnetism and Magnetic Materials, vol. 164, pp. L268-L272, December 1996.